JACS
JOURNAL OF THE AMERICAN CHEMICAL SOCIETY
Article
pubs.acs.org/JACS

Electrochemistry and Electrogenerated Chemiluminescence of Twisted Anthracene-Functionalized Bimesitylenes

Jungdon Suk,[†] Palani Natarajan,[‡] Jarugu Narasimha Moorthy,[‡] and Allen J. Bard*[,†]

[†]Center for Electrochemistry and Department of Chemistry and Biochemistry, The University of Texas at Austin, Austin, Texas 78712, United States

[‡]Department of Chemistry, Indian Institute of Technology, Kanpur 208 016, India

Supporting Information

ABSTRACT: The electrochemistry, spectroscopy, and electrogenerated chemiluminescence (ECL) of a variety of 2- and 4-fold anthracene-functionalized tetraarylbimesityls, **AB1−4**, were investigated. **AB1−4** compounds contain a bimesityl core with 2- and 4-fold anthracene functionalities, which generate a rigid D_{2d}-symmetric structure. Cyclic voltammetry of **AB1** and **AB2** showed two reversible, closely spaced one-electron transfers for both oxidation and reduction, and that of **AB3** and **AB4** showed four reversible, closely spaced one-electron transfers for oxidation and reduction in a benzene/acetonitrile solution. The multielectron transfer properties of all four compounds were confirmed by chronoamperometric experiments with an ultramicroelectrode and digital simulations. These serve as models to probe how interacting groups on a molecule affect the energies of successive electron transfers. **AB1−4** compounds are highly fluorescent in nonaqueous solvents and display blue-green emission. They produce very strong ECL with emission at 480 nm, near that of the photoluminescence spectra that can be assigned to emission by direct formation of the singlet via the S-route.

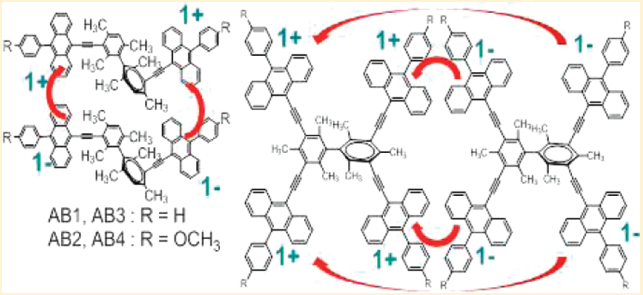

INTRODUCTION

We report here the electrochemical and photophysical characterization as well as radical ion annihilation electrogenerated chemiluminescence (ECL) of a series of twisted anthracene-functionalized bimesitylenes (**AB**s). A series of AB compounds, **AB1−4**, consist of two or four 9-ethynyl-(10-phenyl/*p*-anisyl)anthracene (EA) redox centers linked to a bimesitylene core (B) (Figure 1). Such **AB1−4** compounds are designed for use in organic light-emitting diodes (OLEDs). They show the possibility of a new category of twisted molecules with broader scope and applicability to a new category of amorphous materials for application in OLEDs.[1] The salient features of **AB1−4** are the following: (i) steric repulsion between *o*-methyl groups renders the mesityl rings in bimesitylene core orthogonal; (ii) the vacant meta positions allow ready functionalization to enable facile synthetic accessibility; (iii) amorphous solids are formed (because of the difficulty in undergoing close-packing in the solid state).[2] The methyl groups at the ortho positions of each of the mesitylene rings make the two rings orthogonal and the core rigid. The electronic communication via delocalization, not only between the bimesityl core and the anthracenes but also among the anthracenes, is very small or virtually nonexistent, so that **AB1−4** show interesting electrochemical reductions and oxidations for successive electron-transfer (ET) reactions. They also display the possibility of simultaneous transfers of two (or more) electrons during the annihilation of the reduced and oxidized ions in ECL.

Many organic and organometallic systems produce only a single oxidation or reduction within the accessible potential range of the solvent/electrolyte. Although two separate ET reactions can be observed, addition or removal of a second electron is usually significantly more difficult than the first, because of electrostatic interactions. The separation between the two standard potentials for successive ETs for aromatic hydrocarbons are ~0.5 V, but can vary from 0.1 to >1.0 V because of electronic factors. Depending on the molecular structure, the addition or removal of three, four, five, or six electrons can be detected. For example, C60 and C70[3] undergo stepwise six-electron reductions, and certain polyoxometalate anions[4] have six or more separated one-electron reductions.

Systems that contain two or more identical electroactive groups show various separations between the two potentials, depending on the size of the molecule and degree of delocalization of the charge in the di-ion for a species with two identical electrophores.[5] Savéant et al. proposed that if the effective radius of the localized charge in the electrophore is smaller than the radius of the delocalized charge in the entire molecule, the net solvation energy may be larger and may induce stronger compression of the standard potentials.[6] In the

Received: October 20, 2011
Published: January 17, 2012

dx.doi.org/10.1021/ja209894q | J. Am. Chem.Soc. 2012, 134, 3451−3460

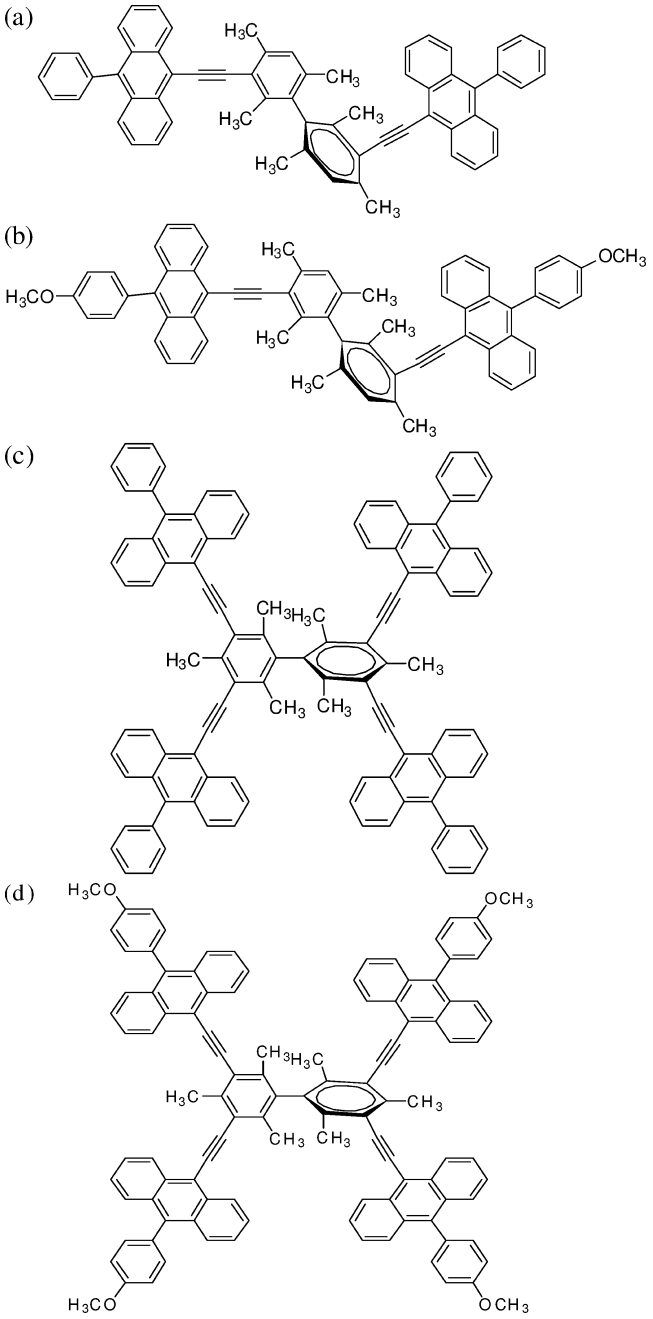

Figure 1. Structure of the 2- and 4-fold anthracene-functionalized bimesityl compounds: (a) **AB1**, (b) **AB2**, (c) **AB3**, and (d) **AB4**.

case of anthracene, the calculated potential difference, $E^{\circ}_1 - E^{\circ}_2$, is 4.187 eV in the gas phase.[7] Addition of the second electron, accounting for solvation energies, decreases the separation to 0.876 V, and ion-pairing effects with the electrolyte further decrease the separation to 0.834 V. In contrast, 2,6-dinitroanthracene shows a significant decrease of $E^{\circ}_1 - E^{\circ}_2$ from 0.834 to 0.137 V.[8] Molecules with two identical electrophores connected by a long saturated chain show a single two-electron wave whose current is exactly double that of a one-electron nernstian wave, characterizing each electrophore as essentially acting independently, except for a statistical factor.[9] This behavior occurs when the two electrophores are independent electronically due to decreasing Coulombic repulsion between the two charges in the dications or dianions. In this case, $E^{\circ}_1 - E^{\circ}_2$ has the statistical limit of (RT/F) ln 4, or 35 mV at 25 °C.[9a,b]

ECL involves the generation of oxidized and reduced species, often radical ions, at electrode surfaces that undergo a fast ET reaction to produce an excited state.[10,11] ECL is produced by directly generating an excited singlet state (S-route) in which the annihilation energy is sufficient to populate the excited singlet state or by triplet−triplet annihilation (T-route) when the energy is not sufficient to populate the singlet state. Another ECL emission mechanism is called the E-route because it results in excimer or exciplex emission.[11] An excimer is an excited-state dimer formed in photoluminescence (PL), by the association of an excited fluorophore with another fluorophore in its ground state.[12] The formation of excimers in ECL by ion annihilation can be a very efficient process when two aromatic systems are brought into proximity.[13] Some dimer and trimer sterically hindered molecules, such as 2,2′-bis(10-phenylanthracen-9-yl)-9,9′-spirobifluorene (**spiro-FPA**),[14] 4,4′-bis(9-(1-naphthyl)anthracen-10-yl)biphenyl (**4A**), and 1,3,5-tris(9-(1-naphthyl)anthracen-10-yl)benzene (**4C**),[15] which show two or three reversible, closely spaced one-electron transfers, produce a second broad emission peak at longer wavelengths in ECL studies, not seen in the PL of the solution. This has been assigned to eximer emission.

Scheme 1 shows the pathways for ECL generation for a representative compound EA∼B∼EA by the radical ion annihilation reaction.

Scheme 1

$$EA{\sim}B{\sim}EA - e^- \rightarrow EA{\sim}B{\sim}EA^{\bullet +} \qquad E^{\circ}_{1,ox} \qquad (1)$$

$$EA{\sim}B{\sim}EA + e^- \rightarrow EA{\sim}B{\sim}EA^{\bullet -} \qquad E^{\circ}_{1,red} \qquad (2)$$

$$EA^{\bullet +}{\sim}B{\sim}EA + EA^{\bullet -}{\sim}B{\sim}EA \rightarrow {}^1EA{\sim}B{\sim}EA^{*} + EA{\sim}B{\sim}EA \qquad (3)$$

$${}^1EA{\sim}B{\sim}EA^{*} \rightarrow EA{\sim}B{\sim}EA + h\nu \qquad (4)$$

However, the closely spaced waves raise the possibility of multiple ET, e.g.,

$$EA{\sim}B{\sim}EA^{\bullet +} - e^- \rightarrow EA^{\bullet +}{\sim}B{\sim}EA^{\bullet +} \qquad E^{\circ}_{2,ox} \qquad (5)$$

$$EA{\sim}B{\sim}EA^{\bullet -} + e^- \rightarrow EA^{\bullet -}{\sim}B{\sim}EA^{\bullet -} \qquad E^{\circ}_{2,red} \qquad (6)$$

and the possibility of simultaneous transfer of two electrons in an annihilation reaction.[14] We describe in this paper the electrochemistry, photophysics, and ECL of a novel set of these twisted anthracene-functionalized bimesitylenes, **AB1−4** compounds. The ion annihilation ECL of **AB1−4** products is described below along with the spectral characterization and the PL and ECL spectra.

EXPERIMENTAL SECTION

Chemicals. The synthesis of **AB1−4**, whose structures are shown in Figure 1, has been described previously.[1] Anhydrous acetonitrile (MeCN, 99.93%) and anhydrous benzene (Bz, 99.9%) were obtained from Aldrich (St. Louis, MO). Tetra-*n*-butylammonium hexafluorophosphate ($TBAPF_6$) was obtained from Fluka and used as received. All solutions were prepared in an Ar atmosphere glovebox (Vacuum Atmospheres Corp., Hawthorne, CA) and placed in an airtight cell with a Teflon cap for measurements completed outside of the box.

Characterization. Electrochemical methods such as cyclic voltammetry (CV), multipotential step voltammetry, and chronoam-

dx.doi.org/10.1021/ja209894q | J. Am. Chem.Soc. 2012, 134, 3451−3460

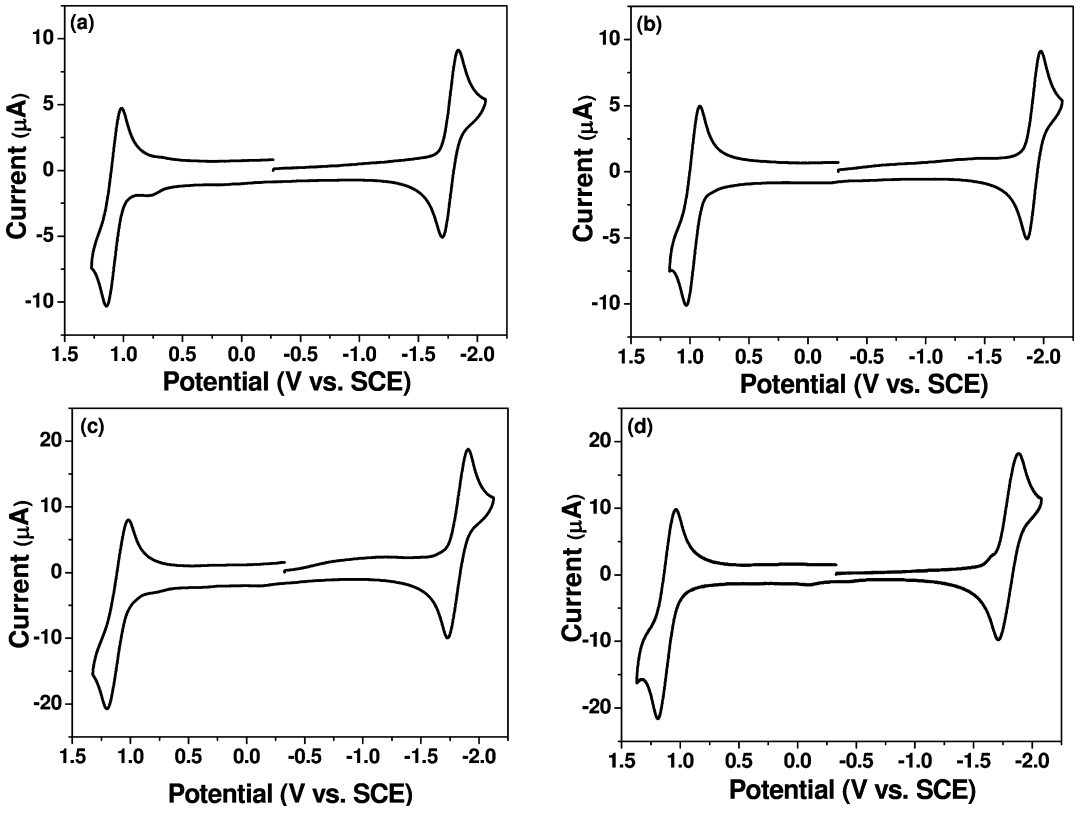

Figure 2. Cyclic voltammograms of 0.5 mM (a) **AB1**, (b) **AB2**, (c) **AB3**, and (d) **AB4** in 3:1 Bz:MeCN with 0.1 M $TBAPF_6$. WE, Pt disk; CE, Pt coil; RE, Ag wire as a QRE; scan rate, 0.5 V/s.

perometry were performed with a three-electrode cell linked to a model 660 electrochemical workstation (CH Instruments, Austin, TX). The electrochemical cell consisted of a Pt wire counter electrode (CE), an Ag wire quasi-reference electrode (QRE), and a 2 mm diameter Pt disk (surface area = 0.0206 cm^2) inlaid in a glass working electrode (WE). The Pt WE was bent at a 90° angle (J-type electrode) so that the electrode surface faced the detector in the ECL experiments. Before each experiment, the WE was polished on a felt pad with 1, 0.3, and 0.05 μm alumina (Buehler, Ltd., Lake Bluff, IL), sonicated in DI water and ethanol for 1 min each, dried in an oven at 100 °C, and then transferred into the glovebox. All potentials were calibrated against saturated calomel electrode (SCE) by the addition of ferrocene as an internal standard at the end of all measurements, taking E°_{Fc/Fc^+} = 0.342 V vs SCE.[16] For chronoamperometry experiments, a 25 μm diameter Pt ultramicroelectrode (UME) was used as a WE. Digital simulations of cyclic voltammograms were performed using DigiSim 3.03 (Bioanalytical Systems, Inc., West Lafayette, IN).

For spectroscopy, all solutions were prepared in a 1 cm quartz cell. UV−vis spectra were recorded with a Milton Roy Spectronic 3000 array spectrophotometer (Rochester, NY). Fluorescence spectra were collected on a QuantaMaster spectrofluorimeter (Photon Technology International, Birmingham, NJ). The relative fluorescence efficiencies were determined with respect to 9,10-diphenylanthracene (DPA) as a standard (λ_{exc} = 380 nm, Φ_{PL} = 0.91 in benzene).[17] ECL transients were simultaneously recorded by an Autolab electrochemical workstation (Eco Chemie, The Netherlands) coupled with a photomultiplier tube (PMT, Hamamatsu R4220p, Japan). The PMT was supplied with −750 V with a Series 225 high-voltage power supply (Bertan High Voltage Corp., Hucksville, NY). ECL transients were generated by pulsing the electrode 80 mV beyond the diffusion-limited peak potentials for oxidation and reduction peaks. For the ECL spectra, the detector was a charge-coupled device camera (Princeton Instruments, SPEC-32). The integration time for all spectra was 3 min, and the slit width was 0.75 μm. The camera was cooled with liquid nitrogen between −100 and −120 °C, and the spectral wavelengths were calibrated using a mercury lamp (Oriel, Stratford, CT). The relative ECL efficiencies were calculated with DPA, with 3:1 Bz:MeCN as a comparison.

RESULTS AND DISCUSSION

Electrochemistry. CV was used to gain information about the electrochemistry of **AB1−4**, to determine the diffusion coefficient, the stability of the radical ions in the solution, and the energies of annihilation reactions in ECL. The CV experiments were carried out in 3:1 Bz:MeCN solutions with 0.1 M $TBAPF_6$ as the supporting electrolyte. CVs of **AB1−4** are shown in Figure 2. The CVs of all four compounds at a scan rate, ν, of 0.5 V/s showed chemically reversible oxidation and reduction waves in the solution. The peak current ratio (i_{pa}/i_{pc}) of the oxidation and reduction waves of all four compounds was essentially unity, indicating the absence of subsequent chemical reactions and good stability of the ions. Moreover, scan rate studies (Supporting Information Figures S1 and S2) showed that the anodic peak current, I_{pa}, and cathodic peak current, I_{pc}, were proportional to the square root of the scan rate ($\nu^{1/2}$), indicating diffusion control for this process; all give diffusion coefficients of $(3.4 \pm 0.2) \times 10^{-6}$ cm^2/s. As shown in Table 1, which reports the peak potentials for the overall multielectron transfer reactions, the trend in the potentials for the oxidation wave is **AB2** < **AB1** and **AB4** < **AB3**. The relative ease of oxidation of **AB2** and **AB4** is a consequence of the presence of methoxy groups in these, although the difference is rather small. The observed separation for the reduction and oxidation peaks for both waves was ∼120 mV, because of uncompensated resistance ($R_u \approx 2700\ \Omega$) and the multielectron transfer nature of

dx.doi.org/10.1021/ja209894q | J. Am. Chem.Soc. 2012, 134, 3451−3460

Table 1. Electrochemical Data

	E_p (V vs SCE)						
chemical	$A/A^{\bullet-}$	$A/A^{\bullet+}$	D ($\times 10^6$ cm^2/s)	total n	E_g[a] (eV)	E_{HOMO}[b] (eV)	E_{LUMO}[c] (eV)
AB1	−1.77	1.08	3.6	2.0	−2.85	−5.84	−2.99
AB2	−1.92	0.97	3.5	2.2	−2.89	−5.73	−2.84
AB3	−1.82	1.11	3.2	4.2	−2.93	−5.87	−2.94
AB4	−1.83	1.07	3.3	4.1	−2.90	−5.83	−2.93

[a]From the CV. [b]The HOMO values are calculated on the basis of the value of −4.8 eV in a vacuum for ferrocene. [c]From the reduction wave.

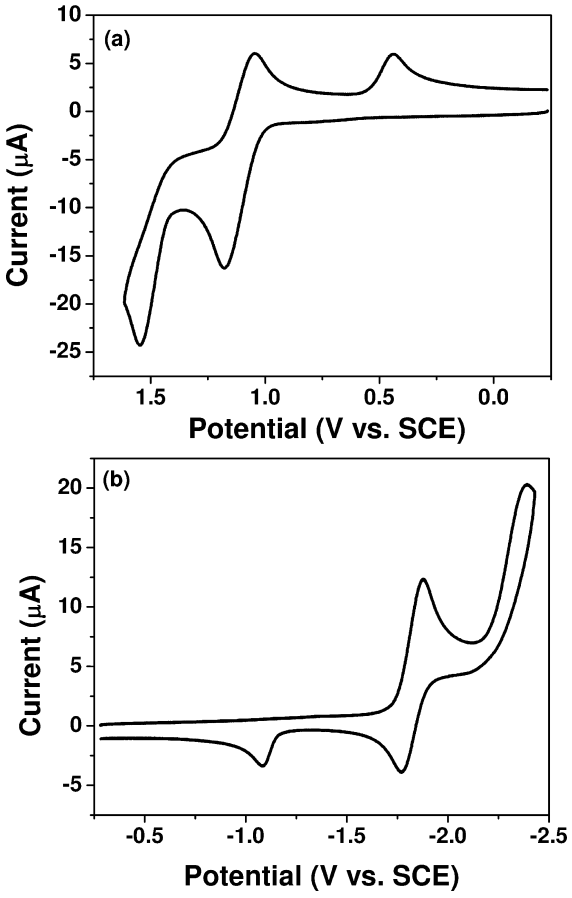

Figure 3. Cyclic voltammograms for (a) oxidation and (b) reduction of 0.5 mM **AB3** in 3:1 Bz:MeCN with 0.1 M $TBAPF_6$. WE, Pt disk; CE, Pt coil; RE, Ag wire as a QRE; scan rate, 0.5 V/s.

the waves. The latter has been confirmed by digital simulation and the chronoamperometric experiments with an UME.

Upon scanning **AB3** to more extreme potentials in both the negative and positive directions, additional waves were observed (Figure 3). The remaining three compounds exhibited similar CV patterns. In all cases, the second waves were chemically irreversible, showing that for **AB1** and **AB2**, for $n > 2$, and for **AB3** and **AB4**, for $n > 4$, the products subsequently undergo rapid reactions. The observed peak separation between the first and second waves was about 590 mV for reduction and 450 mV for oxidation. The large splitting, similar to that for the formation of dianions of many aromatic hydrocarbons[18] and other conjugated organic compounds,[19] is a consequence of the higher repulsion energy for addition (or removal) of electrons into (or from) singly occupied orbitals. The irreversibility of the second reduction and oxidation waves, as with aromatic hydrocarbons, may be due to proton-transfer reactions with impurities in the solvent (e.g., water) or with the supporting electrolyte.[20] Because of primary interest in reactions at the first waves, further study of later waves was not carried out.

As shown by chronoamperometric experiments described below and indicated in Table 1, the first oxidation and reduction waves involve two- (for **AB1** and **AB2**) and four- (for **AB3** and **AB4**) electron transfers. To extract the potentials for the individual ET events, digital simulations of the waves were carried out. In the simulations, all the ET reactions were considered so fast ($k^\circ \geq 10^4$ s^{-1}) that they are diffusion controlled; α values were taken to be 0.5.

Figures 4 and 5 and Supporting Information Figures S3 and S4 show comparisons of experimental and simulated CVs of **AB1** and **AB3** at different scan rates from 50 mV/s to 10 V/s. Digital simulation of CVs with different scan rates yields information about the potentials of the individual reaction steps as well as possible mechanisms for reactions at the electrode. The R_u and double-layer capacitance, c_{dl}, were determined by a potential step at a potential where no faradaic reactions occurred (0.4 V vs SCE), and the simulation was corrected for R_u (2740 Ω) and c_{dl} (600 nF). The fit between the experimental and simulated data for sequential ET mechanisms was good. The oxidation and reduction of **AB1** could be fit by a nernstian two-electron transfer mechanism at all scan rates with sequential ET steps, with potentials of $E^\circ_{1,ox}$ = 1.04 V, $E^\circ_{2,ox}$ = 1.09 V vs SCE (Figure 4) and $E^\circ_{1,red}$ = −1.75 V, $E^\circ_{2,red}$ = −1.78 V vs SCE (Figure 5). The peak separation of **AB1** was about 50 mV on the oxidation side and 30 mV on the reduction side, or an average of ca. 40 mV. The result of fitting between the experimental and simulated oxidation and reduction CVs (Supporting Information Figures S3 and S4) similarly indicated that compound **AB3** had sequential four-electron transfers for the reduction and oxidation waves: $E^\circ_{1,ox}$ = 1.05 V, $E^\circ_{2,ox}$ = 1.09 V, $E^\circ_{3,ox}$ = 1.10 V, $E^\circ_{4,ox}$ = 1.13 V vs SCE and $E^\circ_{1,red}$ = −1.735 V, $E^\circ_{2,red}$ = −1.755 V, $E^\circ_{3,red}$ = −1.785 V, $E^\circ_{4,red}$ = −1.8 V vs SCE, yielding an average difference between successive peaks of 27 mV on oxidation and 22 mV on reduction (25 mV average). Although there is considerable uncertainty in the peak values obtained by simulation, the average values are close to those predicted for the statistical factor without interaction: n = 2, 36 mV; n = 4, 24 mV.[9b] This suggests a lack of interaction among the pendant anthracenyl groups.

The chronoamperometric experiments using an UME were performed for the direct determination of the number of electrons, n, for the first oxidations and reductions without the need to know D.[24] The number of electrons in the oxidation wave was determined by comparing the transient current, $i_d(t)$, and the steady-state current, $i_{d,ss}$, in a chronoamperometric experiment. This method helps to confirm the number of electrons involved in an ET event for **AB1**−**4**. Figure 6a shows the linear scan voltammetry of 0.5 mM **AB3** on a 25 μm radius Pt UME in a 3:1 Bz:MeCN solution with 0.1 M $TBAPF_6$ as the supporting electrolyte. The CV from a Pt UME shows a simple nernstian reaction shape with a clear steady-state current for each oxidation and reduction site. The chronoamperometric

dx.doi.org/10.1021/ja209894q | J. Am. Chem.Soc. 2012, 134, 3451−3460

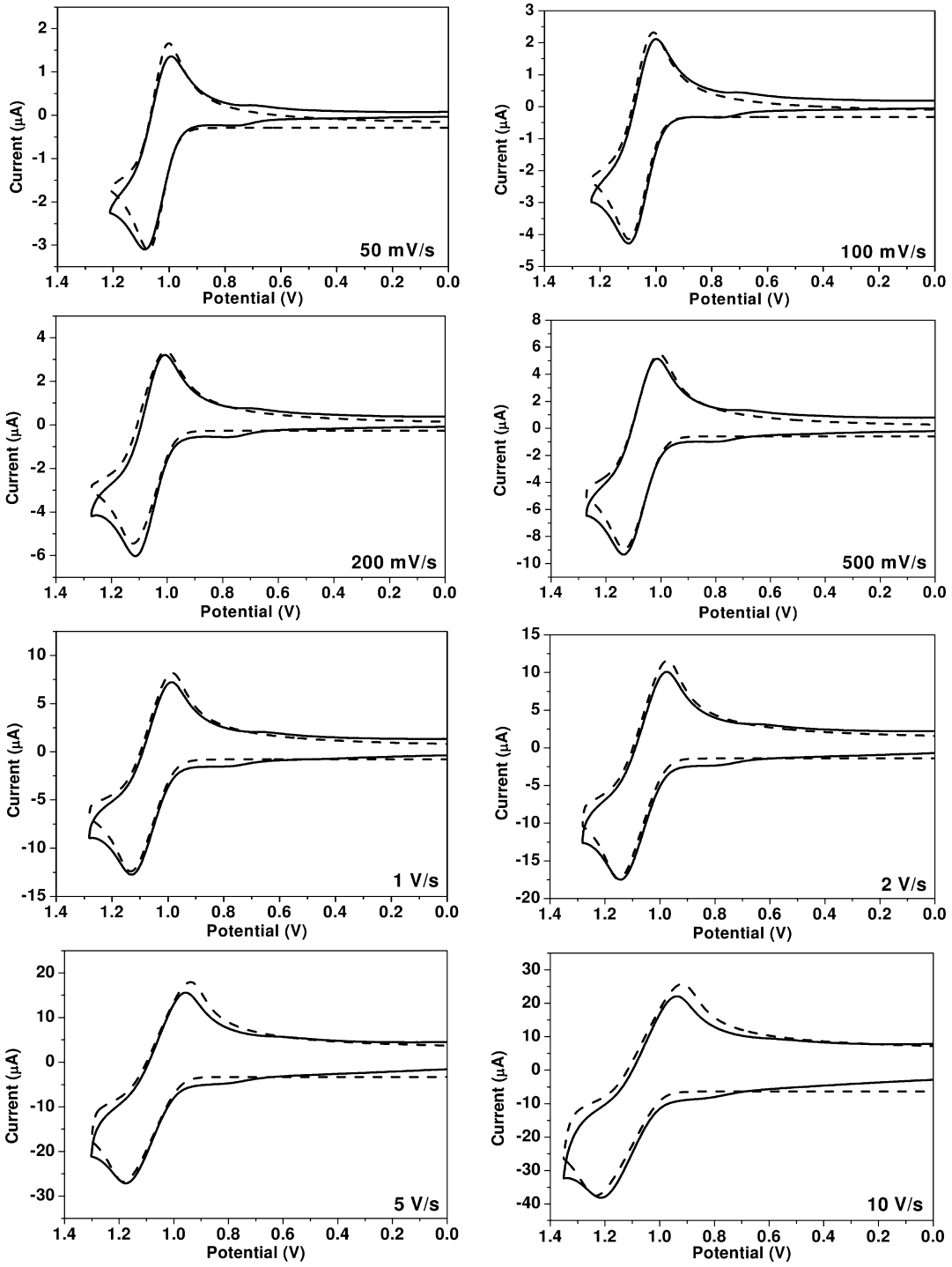

Figure 4. Experimental (solid line) and simulated (dotted line) cyclic voltammograms of 0.5 mM **AB1** oxidation with scan rate from 50 mV/s to 10 V/s. Simulation mechanism is two- and one-electron oxidation and corrected for resistance (2740 Ω) and capacitance (600 nF): $E^{\circ}_{1,ox}$ = 1.04 V, $E^{\circ}_{2,ox}$ = 1.09 V vs SCE, $k^{\circ} > 10^4$ cm/s, α = 0.5.

experiments directly determine the D of a species without knowledge of n and concentration, C^*. The value of D is obtained from the slopes of i–$t^{-1/2}$ curves in chronoamperometry. In the transient region between the double-layer charging and the steady-state regions, a plot of $i_d(t)/i_{d,ss}$ vs $t^{-1/2}$ is linear. Equation 7 shows the relationship between $i_d(t)/i_{d,ss}$ and $t^{-1/2}$.

$$i_d(t)/i_{d,ss} = 0.7854 + (\pi^{1/2}/4)a(Dt)^{-1/2} \quad (7)$$

The linear fit yields a slope of $(\pi^{1/2}/4)a(Dt)^{-1/2}$. This equation is valid in the short time region.[24] After determining D from the slope, n can be calculated using eq 8 for the limiting steady-state current, $i_{d,ss}$, where F is Faraday's constant (96 485 C/mol) and a is the UME radius.[21]

$$i_{d,ss} = 4nFDC^* a \quad (8)$$

Figure 6b shows the experimental ratio $i_d(t)/i_{d,ss}$ against $t^{-1/2}$ for the oxidation of 0.5 mM **AB3** on a 25 μm radius Pt UME

dx.doi.org/10.1021/ja209894q | J. Am. Chem.Soc. 2012, 134, 3451–3460

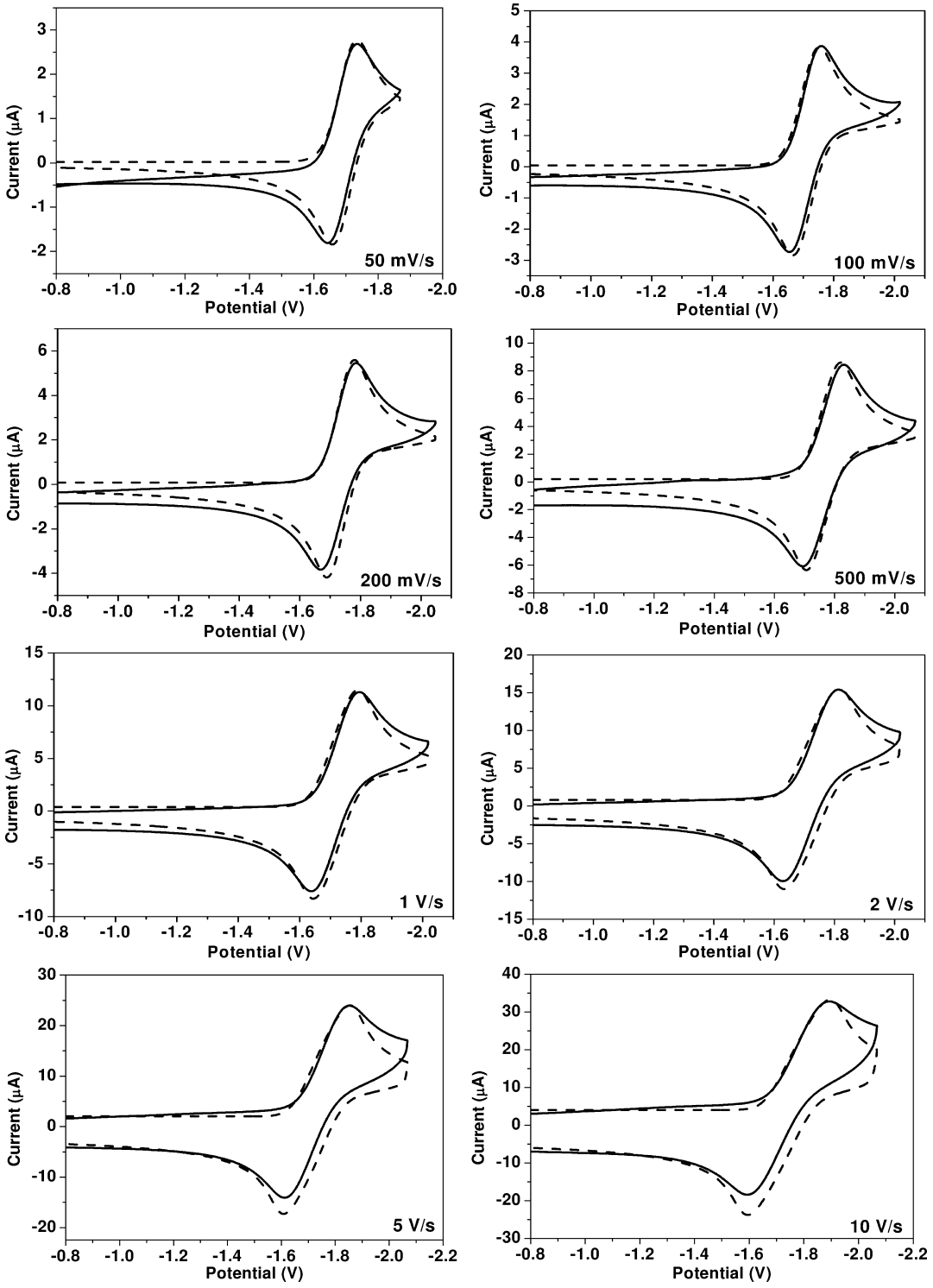

Figure 5. Experimental (solid line) and simulated (dotted line) cyclic voltammograms of 0.5 mM **AB1** reduction with scan rate from 50 mV/s to 10 V/s. Simulation mechanism is two- and one-electron oxidation and corrected for resistance (2740 Ω) and capacitance (600 nF): $E^{\circ}_{1,red} = -1.75$ V, $E^{\circ}_{2,red} = -1.78$ V vs SCE, $k^{\circ} > 10^4$ cm/s, $\alpha = 0.5$.

for the diffusion-controlled UME transient. Linear regression was used to calculate the slope and the intercept over each time region. The diffusion coefficients and n values from the calculations from the chronoamperometry results are shown in Table 1. Overall, both oxidation and reduction of **AB1** and **AB2** involve two electrons, and those of **AB3** and **AB4** involve four-electron transfer processes. The conclusion is that the single oxidation and reduction waves demonstrate that communication via delocalization or electrostatic interaction between the bimesityl core and the two or four anthracene groups as well as between the anthracene functional groups themselves is negligible because the methyl groups cause the two mesitylene rings to be orthogonal and the core rigid.

Spectroscopy. The normalized UV−vis absorption and fluorescence (PL) spectra for **AB1**−**4** are shown in Figure 7; these were obtained in the same solvent as that used for the

dx.doi.org/10.1021/ja209894q | J. Am. Chem.Soc. 2012, 134, 3451−3460

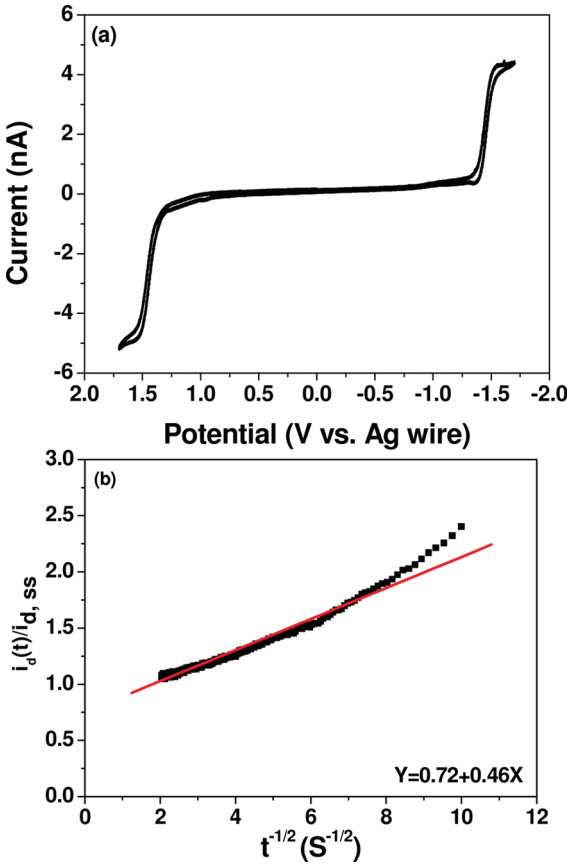

Figure 6. (a) Cyclic voltammogram of 0.5 mM **AB3**. Scan rate, 0.05 V/s. (b) Plot of the experimental ratio $i_d(t)/i_{d,ss}$ against the inverse square root of time for the oxidation of 0.5 mM **AB3**. The sampling ratio is 10 μs per point. The result of the linear regression is also shown. Both experiments were performed in 3:1 Bz:MeCN with 0.1 M $TBAPF_6$. WE, 25 μm diameter Pt microdisc electrode; CE, Pt coil; RE, Ag wire as a QRE.

electrochemical measurement. The optical properties, adsorption and emission maxima, fluorescence quantum yield, and optical energy gap are summarized in Table 2. In general, the UV−vis spectra exhibited absorption bands in the 300−350 and 400−450 nm regions. The strong absorption spectra with several peaks between 300 and 400 nm are assigned to the bands characteristic of anthracene and its derivatives, i.e., the S0 → S1 transition of the anthracene moiety.[22] Compared to anthracene, the emission maxima for **AB1**−**4** are red-shifted by 40−60 nm. **AB2** and **AB4**, with electron-donating *p*-methoxy groups, showed a red-shifted absorption maximum, i.e., a decrease of the singlet gap compared to **AB1** and **AB3**.[23] The fluorescence of these compounds, with excitation at the absorption maxima (~430 nm), showed spectra of **AB1**, **AB3**, and **AB4** with two intense peaks in the 450−480 nm region, corresponding to blue-green emission. The PL spectrum of **AB2** displays an intense emission peak at 460 nm and a broad shoulder at 480 nm. The spectra of **AB1**−**4** showed small Stokes shifts, which suggest little reorganization of the excited states.[24] No PL above 500 nm was observed. The PL quantum yields (Φ_{PL}) for **AB1**−**4** compounds were determined in a Bz:MeCN mixture with DPA as the standard, and the results are recorded in Table 2.

Electrogenerated Chemiluminescence. Figure 8 shows the ECL spectra (dashed line) of **AB1**−**4** compounds in a 3:1 Bz:MeCN mixture containing 0.1 M $TBAPF_6$ during repeated pulsing (pulse width = 0.1 s) between potentials, where the oxidized and reduced forms were alternately produced (with 3 min as the integration time). The potentials were repeatedly stepped from the reduction wave (E_{pc} − 80 mV) to the oxidation wave (E_{pa} + 80 mV), i.e., in the diffusion-limited regions. ECL was initially performed by ion annihilation because the electrochemical results showed that the anions and cations were stable. All compounds produced bright green-blue ECL, which was visible to the naked eye in a dark room. The ECL emissions from **AB1**−**4** had different shapes and maxima compared to their PL spectra. The ECL emission bands of **AB1**−**4** showed an emission maximum around 480 nm. The ECL spectra are frequently a little red-shifted and broader compared with PL spectra. The red-shift in the ECL spectra is attributed to an inner-filter effect because of the difference in the solution concentrations used in PL and ECL measurements, and the broadness is attributed to the difference in the resolution and larger slit width between the different instruments used for spectral measurements.[25] This lower resolution explains why the ECL spectra displayed only one peak (except in the case of **AB2**, which showed a maximum peak at 478 nm and a broad shoulder at 493 nm) compared to the better-resolved PL spectra. Unlike for the molecules previously studied by our group,[14,15] ECL spectra do not show peaks from excimer formation in a longer wavelength region. The bulky mesitylene moieties of the bismesityl core, which force the two rings to adopt an orthogonal configuration and make the overall core rigid, sterically preclude excimer formation.[26] The ECL emission of **AB1**−**4** was very stable for the first 10 min but then gradually decayed and was almost gone after about 6000 s. For comparison, the CVs before and after the ECL decay experiment (Supporting Information Figure S5) clearly show evidence of changes, probably via decomposition of the oxidized and reduced forms.

The enthalpy of the cation and anion annihilation was calculated from the reversible standard potentials of the redox couples with the equation $-\Delta H_{ann} = -\Delta G - T\Delta S = (E^{\circ}_{A^+/A} - E^{\circ}_{A/A^-}) - 0.1$ eV.[11] ΔG was obtained from the difference between the standard potentials of the oxidation and reduction waves in the CVs.[27] The enthalpy of annihilation, $-\Delta H_{ann}$, for **AB1**−**4** compounds calculated from the electrochemical data (shown in Table 2) is larger than the energy for the excited singlet state from the emission spectra, so ECL via the S-route is a good possibility.

To estimate the stability of the ECL and the ionic species, ECL transients for continuous alternating potential pulses were collected, with the potential stepped from the oxidation wave (E_{pa} + 80 mV) to the reduction wave (E_{pc} − 80 mV) with 0.1 or 0.5 s pulse width. During the reduction and oxidation beyond the diffusion-limited peak potentials, the transients are stable for up 5 s, suggesting that the dianion and dication were stable for at least this time. For ECL systems where both radical ions are stable, emission pulses in both the cathodic and anodic directions are essentially equal and stable with time; instability results in larger inequality of the emission pulses and a decay of both anodic and cathodic pulses with time.[28] For example, **AB1** showed symmetrical current pulses and approximately equal ECL emission transients, which shows the redox species are stable (Figure 9), and pulsing ECL transients of **AB2**, **AB3**, and **AB4** showed patterns similar to that of **AB1**. The ECL quantum yields of these AB1 compounds were determined from the number of photons emitted per annihilation event, compared to a

dx.doi.org/10.1021/ja209894q | J. Am. Chem.Soc. 2012, 134, 3451−3460

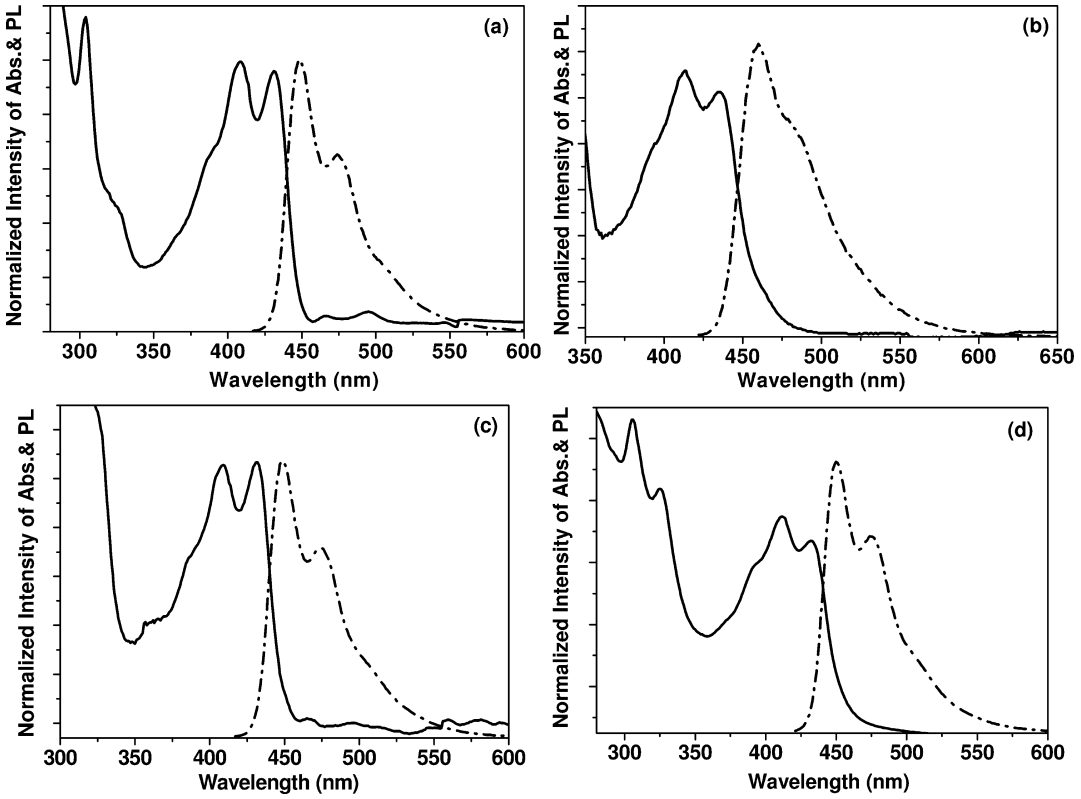

Figure 7. Absorbance spectra (solid line) and fluorescence spectra (dot-dashed line) of (a) **AB1**, (b) **AB2**, (c) **AB3**, and (d) **AB4** in 3:1 Bz:MeCN with 0.1 M $TBAPF_6$. Emission spectra were excited at the absorption maxima.

Table 2. Spectroscopic and ECL Data

chemical	λ_{max}(abs) (nm)	λ_{max}(PL) (nm)	$\Phi_{PL}{}^{a}$	λ_{max}(ECL) (nm)	$\Phi_{ECL}{}^{b}$	$-\Delta G_{ann}{}^{c}$ (eV)	$-\Delta H_{ann}{}^{d}$ (eV)	$E_s{}^{e}$ (eV)
AB1	408, 435	452, 473	0.64	477	0.024	2.85	2.75	2.74
AB2	413, 436	460, 481(s)	0.49	478, 493	0.00087	2.89	2.79	2.69
AB3	408, 431	448, 472	0.65	474	0.035	2.93	2.83	2.74
AB4	413, 436	452, 479	0.68	479	0.00067	2.90	2.80	2.74

[a] Φ_{PL} is the relative PL compared to DPA. $\Phi_{PL,DPA}$ = 0.91 in benzene. [b] Φ_{ECL} is the absolute ECL compared to DPA (taking $\Phi_{ECL,DPA}$ = 0.08).[29] [c] $-\Delta G_{ann} = E_{pa}{}^{ox} - E_{pc}{}^{red}$. [d] $-\Delta H_{ann} = -\Delta G_{ann} - 0.1$. [e] $E_S = 1239.85/\lambda_{max}{}^{PL}$ (nm).

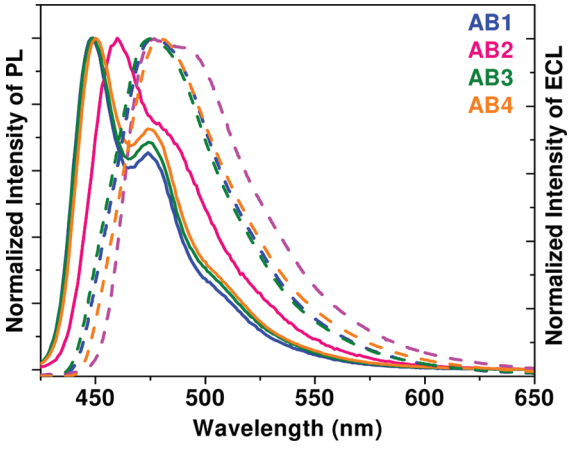

Figure 8. PL spectra (solid line) and ECL spectra (dashed line) of **AB1** (blue), **AB2** (pink), **AB3** (green), and **AB4** (orange) generated by annihilation by stepping between $E_p{}^{red}$ − 80 mV and $E_p{}^{ox}$ + 80 mV. ECL spectra were integrated for 3 min using a 0.75 mm slit width.

standard ECL emitter, DPA. The quantum yield of DPA in acetonitrile has been reported as 8%.[29] This yielded ECL efficiencies of 2.4% for **AB1**, 0.08% for **AB2**, 3.5% for **AB3**, and 0.067% for **AB4**.

As discussed in a previous paper,[14] a one-electron transfer between the dicationic species and the dianionic one would produce an excited state in the presence of radical ions, which should be efficient quenchers of electronic excited states. An alternative possibility is a direct two-electron transfer:

$$EA^{\bullet+}{\sim}B{\sim}EA^{\bullet+} + EA^{\bullet-}{\sim}B{\sim}EA^{\bullet-} \rightarrow {}^{1}EA{\sim}B{\sim}EA^{*}{+}EA{\sim}B{\sim}EA \quad (9)$$

although such reactions have rarely been considered in recent ET studies. Finding a definite mechanism is complicated by the fact that reproportionation reactions can occur, e.g., when the dianion or dication diffuses from the electrode and encounters a flux of parent molecule:

$$EA^{\bullet+}{\sim}B{\sim}EA^{\bullet+} + EA{\sim}B{\sim}EA \rightarrow 2EA^{\bullet+}{\sim}B{\sim}EA \quad (10)$$

$$EA{\sim}B{\sim}EA{+}EA^{\bullet-}{\sim}B{\sim}EA^{\bullet-} \rightarrow 2EA^{\bullet-}{\sim}B{\sim}EA \quad (11)$$

with ECL resulting from reaction of the monoionic species so produced.

dx.doi.org/10.1021/ja209894q | J. Am. Chem.Soc. 2012, 134, 3451−3460

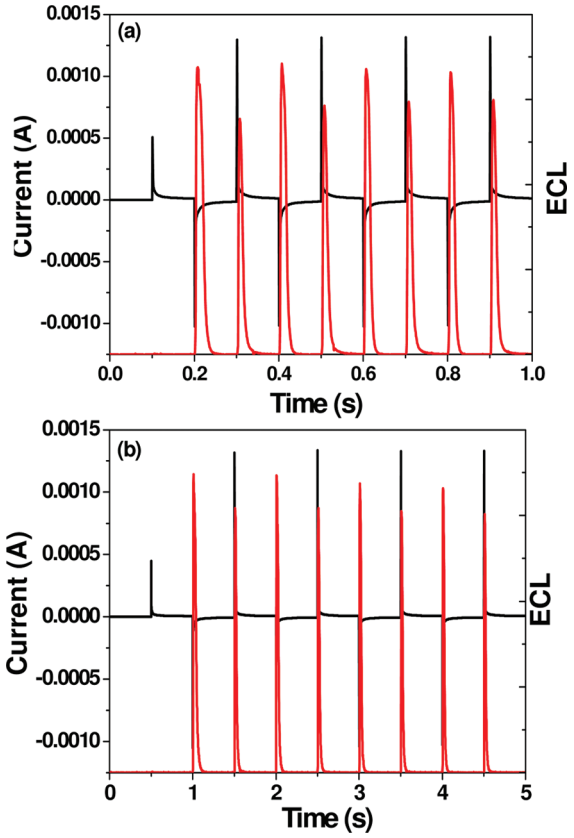

Figure 9. Transient ECL experiment, electrochemical current (black line), and ECL intensity (red line) for **AB1** compound. Sampling time, 1 ms; pulsing pattern, 0 V to negative ($E_{p,\,red}$ − 80 mV) to anodic ($E_{p,\,ox}$ + 80 mV); pulse width, (a) 0.1 or (b) 0.5 s.

CONCLUSION

The electrochemistry and ECL of a novel series of anthracene-functionalized bimesitylenes that are characterized by unique *meta* substitution (**AB3** and **AB4**) and orthogonal planes has been comprehensively investigated. **AB1** and **AB2** with two phenylanthracene redox centers, and **AB3** and **AB4** with four such redox centers, undergo electrochemical processes with a small potential difference (~36 mV for the n = 2 and ~24 mV for the n = 4 species) between the E° values of the successive electron transfers, because the structures preclude delocalization between the anthracene functional groups. Chronoamperometry with an ultramicroelectrode confirmed that the two electrons (n = 2) for compounds **AB1** and **AB2** and four electrons (n = 4) for compounds **AB3** and **AB4** are involved in ET oxidation and reduction. The four compounds show strong photoluminescence at a blue-green wavelength at ~480 nm and produce ECL emission strong enough to be seen with the naked eye.

ASSOCIATED CONTENT

Supporting Information

Additional CVs and simulation results. This material is available free of charge via the Internet at http://pubs.acs.org.

AUTHOR INFORMATION

Corresponding Author

ajbard@mail.utexas.edu

ACKNOWLEDGMENTS

We acknowledge support of this research from Roche Diagnostics, Inc., and J.N.M. is thankful to the Department of Science and Technology, India, for generous financial support.

REFERENCES

(1) Moorthy, J. N.; Venkatakrishnan, P.; Natarajan, P.; Huang, D.; Chow, T. J. *J. Am. Chem. Soc.* **2008**, *130*, 17320.
(2) (a) Natarajan, R.; Savitha, G.; Moorthy, J. N. *Cryst. Growth Des.* **2005**, *5*, 69. (b) Natarajan, R.; Savitha, G.; Dominiak, P.; Wozniak, K.; Moorthy, J. N. *Angew. Chem., Int. Ed.* **2005**, *44*, 2115. (c) Moorthy, J. N.; Natarajan, R.; Venugopalan, P. *J. Org. Chem.* **2005**, *70*, 8568. (d) Moorthy, J. N.; Natarajan, R.; Savitha, G.; Venugopalan, P. *Cryst. Growth Des.* **2006**, *6*, 919.
(3) Xie, Q.; Perez-Cordero, E.; Echegoyen, L. *J. Am. Chem. Soc.* **1992**, *114*, 3978.
(4) Zhang, J.; Bond, A. M.; MacFarlane, D. R.; Forsyth, S. A.; Pringle, J. M.; Mariotti, A. W. A; Glowinski, A. F.; Wedd, A. G. *Inorg. Chem.* **2005**, *44*, 5123.
(5) Evans, D. H. *Chem. Rev.* **2008**, *108*, 2133.
(6) Hapiot, P.; Kispert, L. D.; Konovalov, V.; Savéant, J.-M. *J. Am. Chem. Soc.* **2001**, *123*, 6669.
(7) Fry, A. J. *Electrochem. Commun.* **2005**, *7*, 602.
(8) Macias-Ruvalcaba, N. A.; Telo, J. P.; Evans, D. H. *J. Electroanal. Chem.* **2007**, *600*, 294.
(9) (a) Ammar, F.; Savéant, J.-M. *J. Electroanal. Chem.* **1973**, *47*, 115. (b) Flanagan, J. B.; Margel, S.; Bard, A. J.; Anson, F. C. *J. Am. Chem. Soc.* **1978**, *100*, 4248. (c) Chien, C. K.; Wang, H. C.; Szwarc, M.; Bard, A. J.; Itaya, K. *J. Am. Chem. Soc.* **1980**, *102*, 3100.
(10) Bard, A. J., Ed. *Electrogenerated Chemiluminescence*; Marcel Dekker: New York, 2004.
(11) (a) Faulkner, L. R.; Bard, A. J. In *Electroanalytical Chemistry*; Bard, A. J., Ed.; Dekker: New York, 1977; Vol. *10*, pp 1–95. (b) Faulkner, L. R.; Glass, R. S. In *Chemical and Biological Generation of Excited States*; Waldemar, A., Giuseppe, C., Eds.; Academic Press: New York, 1982; Chapter 6. (c) Richter, M. M. *Chem. Rev.* **2004**, *104*, 3003. (d) Knight, A. W.; Greenway, G. M. *Analyst* **1994**, *119*, 879. (e) Bard, A. J.; Debad, J. D.; Leland, J. K.; Sigal, G. B.; Wilbur, J. L.; Wohlstadter, J. N. In *Encyclopedia of Analytical Chemistry: Applications, Theory and Instrumentation*; Meyers, R. A., Ed.; John Wiley & Sons: New York, 2000; Vol. *11*, p 9842.
(12) (a) Birks, J. B. *Acta Phys. Pol.* **1968**, *34*, 603. (b) Birks, J. B. *Rep. Prog. Phys.* **1975**, *38*, 903.
(13) Bard, A. J.; Park, S. M. In *The Exciplex*; Gordon, M., Ware, W. R., Eds.; Academic Press: New York, 1975; p 275.
(14) Sartin, M. M.; Shu, C.; Bard, A. J. *J. Am. Chem. Soc.* **2008**, *130*, 5354.
(15) Suk, J.; Wu, Z.; Wang, L.; Bard, A. J. *J. Am. Chem. Soc.* **2011**, *133*, 14675.
(16) Sahami, S.; Weaver, M. *J. Electroanal. Chem.* **1981**, *122*, 155.
(17) Stevens, B.; Algar, B. E. *J. Phys. Chem.* **1968**, *72*, 2582.
(18) (a) Hoytink, G. J.; van Schooten, J. *Recl. Trav. Chim. Pays-Bas* **1952**, *71*, 1089. (b) Hoytink, G. J.; van Schooten, J. *Recl. Trav. Chim. Pays-Bas* **1953**, *72*, 903. (c) Hoytink, G. J.; van Schooten, J.; de Boer, E.; Aalbersberg, W. I. *Recl. Trav. Chim. Pays-Bas* **1954**, *73*, 3553. (d) Hoytink, G. J. *Recl. Trav. Chim. Pays-Bas* **1954**, *73*, 895.
(19) (a) Jensen, B. S; Parker, V. D. *J. Am. Chem. Soc.* **1975**, *97*, 5211. (b) Meerholz, K.; Heinze, J. *J. Am. Chem. Soc.* **1989**, *111*, 2325. (c) Millen, K. *Chem. Rev.* **1984**, *84*, 603. (d) Elsenbaumer, R. L.; Shacklette, L. W. In *Handbook of Conducting Polymers*; Skotheim, T. A., Ed.; Marcel Dekker: New York, 1986; p 213.
(20) (a) Aten, A. C.; Buthker, C.; Hoytink, G. J. *Trans. Faraday Soc.* **1959**, *55*, 324. (b) Dietz, R.; Larcombe, B. E. *J. Chem. Soc. B* **1970**, 1369.
(21) Denault, G.; Mirkin, M. V.; Bard, A. J. *J. Electroanal. Chem.* **1991**, *208*, 27.

(22) (a) Jones, N. R. *Chem. Rev.* **1947**, *41*, 353. (b) Nakabayashi, T.; Wua, B.; Morikaw, T.; Iimori, T.; Rubin, M. B.; Speiser, S.; Ohta, N. *J. Photochem. Photobiol. A: Chem.* **2006**, *178*, 236.
(23) Law, K.-Y. *J. Phys. Chem.* **1987**, *91*, 5184.
(24) Reichardt, C. *Solvents and Solvent Effects in Organic Chemistry*; Wiley: New York, 2003.
(25) Sartin, M. M.; Camerel, F.; Ziessel, R.; Bard, A. J. *J. Phys. Chem. C* **2008**, *112*, 10833.
(26) Chandross, E.; Longworth, J.; Visco, R. *J. Am. Chem. Soc.* **1965**, *87*, 3259.
(27) Marcus, R. A. *J. Phys. Chem.* **1989**, *93*, 3078.
(28) Cruser, A.; Bard, A. J. *J. Am. Chem. Soc.* **1969**, *91*, 267.
(29) Keszthelyi, C. P.; Tokel-Takvoryan, N. E.; Bard, A. J. *Anal. Chem.* **1975**, *47*, 249.